Cbln1 accumulates and colocalizes with Cbln3 and GluRδ2 at parallel fiber-Purkinje cell synapses in the mouse cerebellum

Eriko Miura[1], **Keiko Matsuda**[2], **James I Morgan**[3], **Michisuke Yuzaki**[2], and **Masahiko Watanabe**[1]

[1]Department of Anatomy, Hokkaido University School of Medicine, Sapporo 060-8638, Japan

[2]Department of Physiology, School of Medicine, Keio University, Tokyo 160-8582, Japan

[3]Department of Developmental Neurobiology, St. Jude Children's Hospital, Memphis, Tennessee 38105-2794, USA

Abstract

Cbln1 (a.k.a. precerebellin) is secreted from cerebellar granule cells as homohexamer or in heteromeric complexes with Cbln3. Cbln1 plays crucial roles in regulating morphological integrity of parallel fiber (PF)-Purkinje cell (PC) synapses and synaptic plasticity; Cbln1-knockout mice display severe cerebellar phenotypes that are essentially indistinguishable from those in glutamate receptor GluRδ2-null mice and include, severe reduction in the number of PF-PC synapses and loss of long-term depression of synaptic transmission. To understand better the relationship between Cbln1, Cbln3 and GluRδ2, we performed light and electron microscopic immunohistochemical analyses using highly specific antibodies and antigen-exposing methods, i.e., pepsin pretreatment for light microscopy and postembedding immunogold for electron microscopy. In conventional immunohistochemistry, Cbln1 was preferentially associated with non-terminal portions of PF axons in the molecular layer but rarely overlapped with Cbln3. In contrast, antigen-exposing methods not only greatly intensified Cbln1 immunoreactivity in the molecular layer, but also revealed its high accumulation in the synaptic cleft of PF-PC synapses. No such synaptic accumulation was evident at other PC synapses. Furthermore, Cbln1 now came to overlap almost completely with Cbln3 and GluRδ2 at PF-PC synapses. Therefore, the convergence of all three molecules provides the anatomical basis for a common signaling pathway regulating circuit development and synaptic plasticity in the cerebellum.

Keywords

Cbln; GluRδ2; parallel fiber; Purkinje cell; immunohistochemistry; mouse; cerebellum

Introduction

The Cbln family belongs to the C1q/tumor necrosis factor (TNF) superfamily (Shapiro & Scherer, 1998; Bodmer *et al*., 2002; Kishore *et al*., 2004; Bao *et al*., 2005; Yuzaki, 2008), and comprises of Cbln1-Cbln4 that display distinct expression patterns in the brain (Pang *et al*., 2000; Hirai *et al*., 2005; Miura *et al*., 2006a; Wei *et al*., 2007). Cbln1 (a.k.a. precerebellin) was originally identified as a precursor of cerebellum-specific hexadecapeptide cerebellin (Slemmon *et al*., 1984; Urade *et al*., 1991). Cerebellin was isolated from the cerebellum of multiple species from chicken to man (Slemmon *et al*.,

Correspondence to: **Masahiko Watanabe** Department of Anatomy, Hokkaido University School of Medicine, Sapporo 060-8638, Japan. E-mail address, watamasa@med.hokudai.ac.jp.

1984; Burnet *et al.*, 1988; Morgan *et al.*, 1988; Yiangou *et al.*, 1989) where it is concentrated in the synaptosomal compartment (Slemmon *et al.*, 1984) and is reported to undergo depolarization- and calcium-dependent secretion (Burnet *et al.*, 1988). Although biological activities have been ascribed to the cerebellin peptide (Mazzocchi *et al.*, 1999; Albertin *et al.*, 2000; Rucinski *et al.*, 2005), it is now evident that full length, uncleaved Cbln1 is secreted as a hexameric complex (Bao *et al.*, 2005; 2006; Iijima *et al.*, 2007).

Cbln1 is co-expressed with Cbln3 in cerebellar granule cells (Pang *et al.*, 2000; Hirai *et al.*, 2005; Miura *et al.*, 2006a) where they co-exist in the same heteromeric complex (Bao *et al.*, 2006). Moreover, in cultured cells, Cbln3 must associate with Cbln1 in order to exit the endoplasmic reticulum (ER) and undergo trafficking and secretion (Bao *et al.*, 2006; Iijima *et al.*, 2007). Furthermore, genetic elimination of Cbln1 results in a near absence of Cbln3, whereas elimination of Cbln3 results in an ~7-fold increase in Cbln1, indicating that these proteins reciprocally regulate each other's degradation (Bao *et al.*, 2006). Intriguingly, when Cbln3 is co-expressed with Cbln1, it accumulates in the synaptic cleft of Purkinje cell (PC) synapses with parallel fibers (PFs), i.e., granule cell axons (Iijima *et al.*, 2007).

Physiological roles of Cbln1 have been established from neurological and biochemical phenotypes of Cbln1-knockout (KO) mice (Hirai *et al.*, 2005; Bao *et al.*, 2006). The most notable feature is a severe loss of PF-PC synapses; 78% of total PC spines lose synaptic contact. Cbln1-KO mice also display persistent multiple climbing fiber (CF) innervation, impaired long-term depression at the PF-PC synapse, and ataxia. Interestingly, these abnormalities are rapidly rescued by a single injection of recombinant Cbln1 complex (Ito-Ishida *et al.*, 2008), and are essentially the same as those in mutant mice lacking orphan glutamate receptor GluRδ2 (Kashiwabuchi *et al.*, 1995; Kurihara *et al.*, 1997; Landsend *et al.*, 1997; Hashimoto *et al.*, 2001; Lalouette *et al.*, 2001; Ichikawa *et al.*, 2002). These findings suggest that Cbln1 and GluRδ2 may participate in a common mechanism or pathway to promote synapse formation, maintenance, and plasticity.

Here we undertook immunohistochemical localization of Cbln1 using antibodies whose specificity was established using Cbln1-KO mice. We reveal preferential localization of Cbln1 in PF axons and PF-PC synapses and its extensive colocalization with Cbln3 and GluRδ2 at PF-PC synapses, thus providing the basis for anatomical convergence of the Cbln-GluRδ2 signaling pathway.

Materials & Methods

Animals

In the present study, we used adult C57BL and Cbln1-KO mice (Hirai *et al.*, 2005) at 2-3 months of age, which were treated according to the guidelines for the care and use of laboratory animals of Hokkaido University School of Medicine. Under deep pentobarbital anesthesia (100 mg/kg of body weight, i.p.), brains were fixed by transcardial perfusion with 4% paraformaldehyde in 0.1 M sodium phosphate buffer (pH 7.2, PB) for confocal laser scanning microscopy, or with 4% paraformaldehyde/0.1% glutaraldehyde in PB for immunoelectron microscopy. Sections were prepared using a microslicer (50 μm, VT1000S, Leica, Nussloch, Germany).

Antibody

Cbln1 antibodies were raised in the rabbit and guinea pig against synthetic peptide (38-52 amino acid sequence of mouse Cbln1, DSNPTSDPTGTALG, GenBank accession number NM019626) coupled to Keyhole limpet hemocyanin, affinity-purified with the synthetic peptide, and applied to immunohistochemistry and immunoblot. We also used antibodies against the following molecules (species): Cbln3 (rabbit; Iijima *et al.*, 2007), calbindin

(guinea pig and goat; Nakagawa *et al*., 1998; Miura *et al*., 2006b), type-1 and type-2 vesicular glutamate transporters (VGluT1, VGluT2; goat; Miura *et al*., 2006b), synaptophysin (guinea pig; Fukaya *et al*., 2000) and *C*-terminal or intracellular sequence of glutamate receptor GluRδ2 (guinea pig and rabbit; Takeuchi *et al*., 2005). Furthermore, we produced rabbit antibody against *N*-terminal or extracellular sequence (ISALTITPDR, 521-530 amino acids) of GluRδ2 (D13266), which corresponds to the ligand binding H2 site of the S1 segment (Hirai *et al*., 2003). For descriptive convenience, *N*- and *C*-terminal antibodies were termed as GluRδ2*N* and GluRδ2*C* antibodies, respectively, and their specificity was confirmed by selective labeling in the cerebellar molecular layer of control mice and by blank labeling in that of GluRδ2-KO mice (Kashiwabuchi *et al*., 1995; Supplemental Fig. S1). All these primary antibodies were used at 1 μg/ml, unless otherwise noted.

Immunohistochemistry

Throughout experiments, all immunohistochemical incubations were done at room temperature by the free-floating method. For immunofluorescence, phosphate-buffered saline (PBS) containing 0.1% Triton X-100 was used as antibody diluents and washing buffers. Microslicer sections were incubated successively with 10% of normal donkey serum for 20 min, mixtures of primary antibodies overnight, and mixtures of 1:200-diluted Cy3-, Cy5-, and Alexa488-labeled species-specific secondary antibodies for 2 hr (Jackson ImmunoResearch, West Grove, PA; Molecular Probes, Eugene, OR). For nuclear counter staining, sections were incubated with TOTO-3 (Molecular Probes) for 3 min. Photographs were taken with a fluorescence microscope (PROVIS, Olympus Optical, Tokyo, Japan), using a 4x (UplanApo, NA = 0.16) objective lens, and or confocal laser scanning microscope (FV1000, Olympus), using a 40x (UPlanFL N, NA = 1.30) or 60x oil immersion objective lens (PlanApo N, NA = 1.42). Cy3, Alexa488, or Cy5 was excited with a 488, 543, or 633 nm laser beam, and observed through 500-530 nm, 555-625 nm, or > 650 nm emission filters, respectively. For pepsin pretreatment, microslicer sections were treated, prior to normal serum blocking, with 1 mg/ml pepsin (Dako, Carpinteria, CA) in 0.2 N HCl at 37 °C for 3 min.

For silver-enhanced preembedding immunogold electron microscopy, microslicer sections were dipped in 5% bovine serum albumin (BSA)/0.02% saponin/PBS for 30 min, incubated overnight with Cbln1 antibody (0.1 μg/ml) diluted with 1% BSA/0.005% saponin/Tris-buffered saline (TBS, pH 7.5), and subjected to silver-enhanced immunogold labeling using anti-rabbit IgG conjugated with 1.4 nm gold particles (Nanogold; Nanoprobes Inc., Stony Brook, NY, USA) and silver enhancement kit (HQ silver; Nanoprobes Inc.). Sections were further treated with 1% osmium tetroxide and 2% uranyl acetate, and embedded in Epon 812. Ultrathin sections (70 nm in thickness) were prepared with an ultramicrotome (Leica, Wien, Austria), and photographs were taken with an H7100 electron microscope (Hitachi, Tokyo, Japan).

For postembedding immunogold electron microscopy, microslicer sections (300 μm in thickness) were cryoprotected with 30% sucrose/PB and frozen rapidly with liquid propane in an EM CPC unit (Leica). Frozen sections were immersed in 0.5% uranyl acetate in methanol at -90 °C in an AFS freeze-substitution unit (Leica), infiltrated at -45 °C with Lowicryl HM-20 resin (Lowi, Waldkraiburg, Germany), and polymerized with UV light. After etching with saturated sodium-ethanolate solution for 3 sec, ultrathin sections on nickel grids were treated successively with 2% human serum albumin (Wako, Osaka, Japan)/0.1% Tween 20 in Tris-buffered saline (pH 7.5) (HTBST) for 30 min, rabbit Cbln1 antibody (30 μ/ml) or GluRδ2 antibody (20 μ/ml) in HTBST overnight, and colloidal gold (10 nm)-conjugated anti-rabbit IgG (1:100; British Bio Cell International, Cardiff, UK) in

HTBST for 2 hr. Finally, grids were stained with 2% uranyl acetate for 20 min and mixed lead solution for 30 sec. Photographs were taken with an H-7100 electron microscope.

The density and distribution of immunogold particles were quantitatively analyzed on electron micrographs using IPLab software (Nippon Roper, Tokyo, Japan) (n = 2 mice). The density of Cbln1 on synaptic and extrasynaptic membranes of PC synapses were calculated by measuring the number of immunogold particles that were apart less than 35 nm from the cell membrane and the length of measured cell membranes. Perpendicular distribution of Cbln1 or GluRδ2 at PF-PC synapses was examined by sampling synaptic profiles whose presynaptic and postsynaptic membranes were cut perpendicularly to the plane of the synaptic cleft and by measuring the distance from the midline of the synaptic cleft to the center of immunogold particles. Because results from two mice were very similar, data were pooled to compare the labeling density and to construct the distribution histogram. For statistical analysis, data were analyzed using an unpaired Student's *t* test. Statistical significance was assumed when $p < 0.05$.

Expression of recombinant Cbln cDNAs in heterologous cells

Human embryonic kidney 293 (HEK293) cells (a kind gift of Dr. R. Horn, Thomas Jefferson University Medical School, Philadelphia, USA) were cultured in Dulbecco's modified Eagle's medium (DMEM; Invitrogen, Carlsbad, USA) supplemented with 10% fetal calf serum and L-glutamine (1 mM) and grown in 10% CO_2 at 37 °C. We added cDNA encoding hemagglutinin (HA) to the 5' end of the Cbln1-Cbln4; the sequence was then added to the 3' end of the signal sequence by a standard PCR-based mutagenesis with Pyrobest PCR polymerase (Takara bio, Otsu, Japan). The cDNAs were cloned into the pCAGGS expression vector (provided by Dr. J. Miyazaki, Osaka University, Japan) and transfected into HEK293 cells using CellPhect (GE Healthcare Bio-Sciences, Piscataway, USA).

Subcellular fractionation and immunoblot analysis

Cerebellum was homogenized in 0.32 M sucrose in buffer A (10 mM Tris-HCl and 1 mM EDTA, pH 7.5), and centrifuged at $800 \times g$ for 5 min. The supernatant (S1) was centrifuged at $12,000 \times g$ for 15 min. The resulting supernatant (S2) and pellet (P2), which was resuspended in buffer A, were centrifuged at $25,000 \times g$ for 15 min to yield the LP1, LS, P3, and S3 fractions as described (Huttner *et al*., 1983). The postsynaptic density (PSD) fraction was obtained from the LP1 fraction after incubation with 1% Triton X-100 in PBS for 1 h at 4 °C, followed by centrifugation at $100,000 \times g$ for 30 min. Ten micrograms of proteins in each fraction were subjected to sodium dodecyl sulfate-polyacrylamide gel electrophoresis (SDS-PAGE) followed by the immunoblot analysis using antibodies to Cbln1, GluRδ2, synaptophysin (Sigma), or BiP (BD Biosciences, San Jose, USA).

Results

Specificity of Cbln1 antibody and immunohistochemistry

Affinity-purified polyclonal antibodies were produced in the rabbit and guinea pig against amino acid residues 38-52 of the mouse Cbln1, because of its low sequence homology to the other three isoforms (Fig. 1A). In the brain, Cbln1 antibodies of both species predominantly labeled the cerebellum (Fig. 1B). The pattern of immunolabeling disappeared almost completely in the brain of Cbln1-KO mice (Fig. 1C), or with use of the antibody preabsorbed with antigen peptides (Fig. 1D). Furthermore, Cbln1 antibodies detected HEK293 cells expressing Cbln1, but not those expressing Cbln2-Cbln4 (Fig. 1E). These results indicate that the Cbln1 antibodies specifically recognize endogenous and recombinant Cbln1 by immunohistochemical analysis. Because rabbit Cbln1 antibody showed a lower background labeling than the guinea pig one, we therefore used the rabbit

antibody for subsequent analyses and the guinea pig antibody only for Cbln1 and Cbln3 double labeling studies (Fig. 7A-C, E, and F).

Distribution of Cbln1 in the cerebellum

In the cerebellum, Cbln1 was detected as tiny puncta distributed moderately in the molecular layer (red in Fig. 2A and C) and weakly in the granular layer (red in the Fig. 2D). No such labeling was detected in the cerebellum of Cbln1-KO mice (Fig. 2B). By double immunofluorescence for calbindin, a marker for PCs in the cerebellum, Cbln1 was not detected inside calbindin-positive somata, dendrites, or spines (Fig. 2C). Instead, Cbln1 was distributed around calbindin-positive PC dendrites and spines. In the granular layer, punctate immunolabeling for Cbln1 was found in perikarya of granule cells containing TOTO-3-stained round nuclei (arrowheads in Fig. 2D), and also around synaptophysin-positive nerve terminals in the cerebellar glomerulus (arrows in Fig. 2D). Thus, Cbln1 is richly distributed in the neuropil of the molecular layer with relatively lower abundance in the granular layer.

Effects of pepsin pretreatment on Cbln1 immunofluorescence

We found that Cbln1 immunolabeling in the molecular layer was further intensified after section pretreatment with pepsin (Fig. 3A and B), which has been developed to unmask epitopes of synaptic molecules, such as ionotropic glutamate receptors and their scaffolding proteins in the PSD (Watanabe *et al.*, 1998; Fukaya & Watanabe, 2000). In order to determine subcellular distribution of Cbln1 appearing after pepsin pretreatment, cerebellar molecular layer was examined at high magnifications by multiple immunofluorescence labeling (Fig. 3C-F). Without pepsin pretreatment, relatively weak immunofluorescent signals for Cbln1 were detected in VGluT1-positive PF terminals (arrows in Fig. 3C), whereas intense Cbln1 puncta (arrowheads in Fig. 3C) were juxtaposed to but not overlapped with either VGluT1 or calbindin. After pepsin pretreatment, intensified Cbln1 puncta came to overlap more with VGluT1 and calbindin, and were often interposed between them (arrows in Fig. 3D). Furthermore, the intensified Cbln1 puncta displayed almost complete overlap with GluRδ2 (arrows in Fig. 3E). Cbln1-positive puncta, however, showed no apparent overlap in or apposition to VGluT2-positive CF terminals (Fig. 3F). These results suggest that Cbln1 is mainly distributed in and around PF terminals in the molecular layer, and that its large amounts seem to accumulate at PF-PC synapses in an *antigen-hidden* manner.

Preembedding immunogold for Cbln1

To verify this possibility, we first employed preembedding silver-enhanced immunogold electron microscopy. Most metal particles for Cbln1 were detected in non-terminal portion of PFs, and a few were in PF terminals and PC spines (Fig. 4A and B). Of these elements, immunogold particles were preferentially associated with the extracellular surface of the cell membrane, and cytoplasmic labeling was very rare. To quantitatively evaluate this distribution, the density of immunogold particles was measured in these elements. The highest labeling density was observed in non-terminal portion of PF axons, whose level was several times higher than the background level as determined from the same element of Cbln1-KO mice (Fig. 4C). The percentage of cell membrane-associated labeling was 94% of the total labeling in non-terminal PF axons. On the other hand, the density in PF terminals was double the background level, and that in PC spines was around the background level. Preembedding immunogold analysis thus reveals cell membrane-associated localization of Cbln1, particularly, in non-terminal portion of PF axons, which likely corresponds to intense puncta in VGluT1-negative elements (Fig. 3C). In contrast to cell surface labeling in the molecular layer, metal particles in the granular layer were mainly found intracellularly in granule cell perikarya (arrows in Fig. 4D).

Considering remarkable intensification at putative PF-PC synapses after pepsin pretreatment (Fig. 3D and E), we judged that preembedding immunogold microscopy still failed to detect synaptic Cbln1.

Postembedding immunogold for Cbln1 and GluRδ2

Then, we employed postembedding immunogold electron microscopy, which often effectively detects molecular epitopes condensed at synaptic sites (Ottersen and Landsend, 1997; Fukaya *et al*., 2006; Fig. 5 and 6). Labeling for Cbln1 was preferentially detected along the synaptic membrane, or in the synaptic cleft, of PF-PC synapses, whereas that on the peri-and extrasynaptic membranes of PF terminals was very rare (Fig. 5A and B). This was confirmed by quantification of immunogold labeling. Among terminal membranes of PFs, the density of immunogold particles was highest in the synaptic membrane, whose level was significantly higher than the background level as determined from PF-PC synapses of Cbln1-KO mice ($p = 2.897 \times 10^{-10}$, unpaired Student's *t* test; Fig. 5C and 6A), whereas that in the perisynaptic and extrasynaptic membranes were considerably low. In contrast, labeling densities at the CF-PC (Fig. 5E) and interneuron-PC (Fig. 5F) synapses were almost similar to the background level ($p = 0.940$ and 0.885, respectively, unpaired Student's *t* test; Fig. 6A). PF synapses onto molecular layer interneurons showed moderate labeling, but this labeling was not statistically significant as compared with the background level ($p = 0.063$, unpaired Student's *t* test).

Such a preferential and almost selective labeling of the PF-PC synapse quite resembled the case of GluRδ2 (Landsend *et al*., 1997; Takeuchi *et al*., 2005; Fig. 5D). Then we compared the vertical distribution of Cbln1 with that of GluRδ2 at PF-PC synapses (Fig. 6B). The peak of distribution of Cbln1 immunogold particles was found at the midline bin, i.e., -5~+5 nm bin (minus and plus represent presynaptic or postsynaptic side, respectively, from the midline), and labeling declined steeply as being apart from the midline toward both sides. The average vertical position of Cbln1 immunogold particles was -0.86 ± 51.56 nm (mean ± SD, n = 1145 particles) from the midline of the synaptic cleft. As to GluRδ2, we used two antibodies against extracellular and intracellular epitopes: GluRδ2*N* and GluRδ2*C* antibodies. The distributions of GluRδ2*N* and GluRδ2*C* immunogold particles were both peaked at +5~+15 nm bin (Fig. 6B), and the average vertical position was $+4.86 \pm 16.89$ nm for GluRδ2*N* (n = 690 particles) or $+10.49 \pm 27.20$ nm for GluRδ2*C* (n = 709 particles). The mean width of the synaptic cleft, being determined from sampled synapses as the distance between the outer leaflets of presynaptic and postsynaptic membranes, was 15.03 ± 3.20 nm (n = 238 synapses). Taking the width into consideration, the averaged epitope positions detected by GluRδ2*N* and GluRδ2*C* antibodies fall into the synaptic cleft of PF-PC synapses or intracellular site of PC spines, respectively, as expected. In this regard, it should be noted that the average epitope position of Cbln1 is at the middle of the synaptic cleft, and is close to the extracellular epitope of GluRδ2. Furthermore, subcellular fractionation analysis revealed that Cbln1 and GluRδ2 were colocalized with mostly in the synaptosomal (or P2) and PSD fractions (Supplemental Fig. S2). Together, these findings indicate that Cbln1 is preferentially recruited to PF-PC synapses among PC synapses, as is the case for GluRδ2 (Landsend *et al*., 1997).

Colocalization of Cbln1 and Cbln3 at PF-PC synapse

In addition to Cbln1, Cbln3 is also expressed in cerebellar granule cells (Pang *et al*., 2000; Miura *et al*., 2006a), and accumulates in the synaptic cleft of PF-PC synapses in an antigen-hidden manner (Iijima *et al*., 2007). In this study, we compared the distribution of Cbln1 and Cbln3 by double immunofluorescence with or without pepsin pretreatment (Fig. 7). Without the pretreatment, staining for Cbln3 was very high in the granular layer, while it was very low in the molecular layer, as being opposite to Cbln1 (Fig. 7A). Such a contrasting

distribution was also true at high magnification; most, if not all, Cbln1 and Cbln3 formed distinct molecular clusters in both the granular (Fig. 7B) and molecular (Fig. 7C) layers. Preembedding immunogold electron microscopy revealed that Cbln3 was distributed inside perikarya of granule cells, where metal particles were often associated with the ER and nuclear envelope (Fig. 7D). After pepsin pretreatment, immunoreactivity for Cbln3 was strikingly elevated and became punctuate in the molecular layer (Fig. 7E). As a result, Cbln3-positive puncta were almost completely overlapped with Cbln1 (arrows in Fig. 7F) and GluRδ2 (arrows in Fig. 7G). Therefore, Cbln1 is preferentially enriched and colocalized with Cbln3 at the PF-PC synapse.

Discussion

Cbln1 mRNA is predominantly expressed in the brain (Miura *et al*., 2006a), where it is highly expressed in cerebellar granule cells (Pang *et al*., 2000; Hirai *et al*., 2005; Miura *et al*., 2006a). In the present study, we examined its protein distribution in the adult mouse cerebellum by producing polyclonal antibodies specific to Cbln1 and by employing antigen-exposing methods for immunofluorescence and immunoelectron microscopy. Here we have disclosed its enriched distribution in the molecular layer, preferential localization in PF axons and synapses, and extensive colocalization with Cbln3 and GluRδ2 at PF-PC synapses.

Comparison with reported Cbln1 immunolocalization

These immunohistochemical patterns differ to varying degrees from those reported in previous studies. Using antisera against synthetic cerebellin peptide, earlier reports showed its exclusive distribution inside PC elements, most prominently in dendrites and spines although also in the soma (Slemmon *et al*., 1985; Morgan *et al*., 1988; Mugnaini *et al*., 1988). This cellular distribution of cerebellin peptide, though apparently contradictory to that of Cbln1 in the present study, is interesting in that cerebellin peptide levels in the cerebellum correlate with the formation of PF-PC synapses (Slemmon *et al*., 1985), the peptide is concentrated in the synaptosome fraction (Slemmon *et al*., 1984; Burnet *et al*., 1988), and its levels are depleted in the spontaneous cerebellar mutant mice, *reeler, staggerer,* and *weaver* (Slemmon *et al*., 1988). One possibility is that the antibody used here recognizes full length Cbln1 that is secreted in an uncleaved form still harboring the cerebellin sequence, whereas the cerebellin antisera only recognize the fully processed peptide and not the precursor. In this scenario, the antibody used here, raised against amino acid residues 38-52, recognizes the Cbln1-containing complexes in the secretory pathway in granule cells and PF-PC synapses, whereas the earlier cerebellin peptides detect the location of the hexadecapeptide after the extensive proteolytic processing known to occur *in vivo* (Bao *et al*., 2005). If so, the different cellular distribution between the present and previous studies may reflect transneuronal transport and metabolism of Cbln1.

Punctate Cbln1 labeling in granule cell perikarya (Fig. 2D and 4D) is consistent with a recent study by Wei *et al*. (2007), using a highly specific antiserum to the C1q domain of Cbln1. In that study, Cbln1 was enriched in the endolysosomal compartment, which may be a reflection of the proteolytic processing of Cbln1 (Bao *et al*., 2005). However, we found much more intense Cbln1 immunoreactivity in the molecular layer than in the study by Wei *et al*. (2007). Again, although we cannot at present offer a clear explanation for these partially different labeling patterns, our data provide compelling evidence for the specificity of Cbln1 labeling at PF-PC synapses. This finding suggests novel Cbln1-mediated function and mechanisms, as discussed below.

Cbln1 complexes efficiently accumulate at PF-PC synapse

We have previously shown preferential accumulation of Cbln3 at PF-PC synapses by postembedding immunogold microscopy (Iijima *et al*., 2007). In the present study, we demonstrated by pepsin-pretreated immunofluorescence and postembedding immunogold techniques that Cbln1 selectively accumulated at the PF-PC synapse among all PC synapses (Fig. 6A) and colocalized with Cbln3 (Fig. 7E and F). At this synapse, the vertical position of Cbln1 epitopes (0.86 ± 2.21 nm presynaptic to the midline) is very close to that Cbln3 epitopes (1.44 ± 2.27 nm presynaptic), as calculated in the present study from the histogram published by Iijima *et al*. (2007). Considering the fact that Cbln1 interacts with and is co-released with Cbln3 (Pang *et al*., 2000; Bao *et al*., 2006; Iijima *et al*., 2007), the extensive colocalization and proximity of Cbln1 and Cbln3 epitopes provide anatomical support for the existence of heteromeric Cbln1/Cbln3 complexes being at PF-PC synapses. Without pepsin pretreatment, Cbln1 and Cbln3 were detected in distinct molecular clusters abundant in the molecular or granular layer, respectively (Fig. 7A-C). The preembedding immunogold method localized Cbln1 to the extracellular surface of PF axons and terminals (Fig. 4), and Cbln3 to the ER and nuclear envelop of granule cell perikarya (Fig. 7D). These observations *in vivo* suggest that homomeric Cbln1 complex can be released extracellularly but homomeric Cbln3 complexes (if they can form at all) and monomers remain in granule cells, and further that the formation of heteromeric Cbln1/Cbln3 complexes greatly promotes synaptic recruitment and/or anchoring. The former notion is consistent with the biochemical finding that release of Cbln3 requires the interaction with Cbln1 to exit the ER or *cis*-Golgi, whereas Cbln1 by itself can be released into the extracellular space (Bao *et al*., 2006; Iijima *et al*., 2007).

Exogenous application of recombinant homomeric Cbln1 complexes to Cbln1-null PCs in culture leads to accumulation of synaptophysin-positive presynaptic terminals onto PC spines, and a single injection of the complexes into the subarachnoid supracerebellar space in Cbln1-null mice rescues severe ataxia and restores PF-PC synapse formation (Ito-Ishida *et al*., 2008). Furthermore, Cbln3-null mice have no ataxia and display normal rotarod performance (Bao *et al*., 2006). Considering these lines of evidence, it is assumed that homomeric Cbln1 complexes *per se* can accumulate at PF-PC synapses and exert their physiological function. Taken altogether, exclusive synaptic labeling for Cbln1 and Cbln3 should reflect preferential accumulation of homomeric and heteromeric Cbln1 complexes at the PF-PC synapse. In this regard, binding of hexameric Cbln1 homomer and Cbn1/Cbln3 heteromer to PF-PC synapses needs to be tested.

Cbln1 and Cbln3 are colocalized with GluRδ2 at the PF-PC synapse

Striking improvement by antigen unmasking methods in immunohistochemical detection of synaptic Cbln1 and Cbln3 and of the *N*-terminus of GluRδ2 further highlights that the synaptic cleft is one of the neuronal sites with intense protein-protein interaction, as is known for the PSD and axon initial segment (Watanabe *et al*., 1998; Fukaya *et al*., 2006; Lorincz & Nusser, 2008). Anatomically, the synaptic cleft is not an electron-lucent space, but is filled with electron-dense materials that bridge presynaptic and postsynaptic membranes (Takeuchi *et al*., 2005). From the molecular perspective, various adhesion molecules, such as cadherins, protocadherins, neuronligins, and neurexins, are present in the synaptic cleft to regulate pre- and postsynaptic differentiation, molecular organization, synaptogenesis, synaptic adhesion and matching, and synaptic function and plasticity (Craig & Kang, 2007; Shapiro *et al*., 2007). Various neurotransmitter receptors also expose their extracellular domains to the synaptic cleft to mediate ligand binding and initial subunit dimerization (Stern-Bach *et al*., 1994; Kuusinen *et al*., 1995; Laube *et al*., 1997; Ayalon & Stern-Bach, 2001). Intriguingly, the first *N*-terminal 92 amino acids of α-amino-3-hydroxy-5-methyl-4-isoxazone propionic acid (AMPA)-type glutamate receptors have been

shown to directly interact with N-cadherin, promote the formation and growth of dendritic spines, and stimulate presynaptic development and function in hippocampal neurons (Passafaro *et al*., 2003; Saglietti *et al*., 2007).

Mutant mice lacking Cbln1 or GluRδ2 share common phenotypes (Watanabe, 2008; Yuzaki, 2008). These include free PC spines caused by failed synaptic contact with PFs, mismatching of pre- and postsynaptic differentiations at PF-PC synapses, impaired long-term depression at the PF-PC synapse, distal extension of CF innervation territory, persistence of multiple CF innervation, and severe ataxia (Guastavino *et al*., 1990; Kashiwabuchi *et al*., 1995; Kurihara *et al*., 1997; Hashimoto *et al*., 2001; Lalouette *et al*., 2001; Ichikawa *et al*., 2002; Takeuchi *et al*., 2005; Hirai *et al*., 2005; Ito-Ishida *et al*., 2008). In addition, Cbln1, like GluRδ2 (Landsend *et al*., 1997), selectively accumulates at PF-PC synapses (Fig. 5 and 6A). These similarities, together with the analogy to the synapse forming activity of AMPA receptor subunits, raise the possibility that the *N*-terminus of GluRδ2 might interact with Cbln1 complexes in the synaptic cleft of PF-PC synapses, either directly or indirectly, to promote synapse formation, differentiation, and maturation. Alternatively, because the proinflammatory cytokine TNFα, a member of the C1q/TNF superfamily, is known to participate in AMPA receptor trafficking and regulate activity-dependent homeostatic scaling of excitatory synaptic transmission (Stellwagen and Malenka, 2006; Ferguson et al., 2008), Cbln1 might regulate synaptic connectivity through such modulation of synaptic excitability.

Cbln1 is primarily associated with the surface of PF axons and synapses

The preembedding immunogold method revealed the highest labeling for Cbln1 on the outer surface of PF axons (Fig. 4C), while the postembedding immunogold method uncovered a concentrated localization in the synaptic cleft of PF-PC synapses and moderate labeling at PF-interneuron synapses (Fig. 5F and 6A). These findings suggest that, after secretion, Cbln1 complexes are primarily associated with the surface of PF axons and synapses, although the Cbln family lacks a transmembrane domain (Yuzaki, 2008). Other members of the C1q/TNF superfamily also exhibit membrane-associated distribution, such as C1q (Kaul *et al*., 1995), C1q related factor or C1ql1 (Berube *et al*., 1999), TNF ligands (Kishore *et al*., 2004), and C1qTNF1/G-protein coupled receptor interacting protein (Innamorati *et al*., 2002). Thus, it is possible to assume that certain presynaptic mechanisms mediate specific association of Cbln1 complexes with PFs, and that such mechanisms would contribute to selective recruitment to the PF synapse of particular postsynaptic molecules in PCs, such as GluRδ2 and delphilin (Miyagi *et al*., 2002;Takeuchi *et al*., 2008). In turn, the recruitment of particular postsynaptic molecules could further recruit particular presynaptic molecules in PFs, such as Cbln1 and Cbln3, to the PC synapse. The validity of this assumption to explain the characteristic localization of Cbn1 and its functional significcance in cerebellar development and physiology should be tested in future studies.

In conclusion, the present study has revealed for the first time that Cbln1 accumulates at high levels at the PF-PC synapse along with Cbln3 and GluRδ2. This finding will be the anatomical basis for future studies on the molecular mechanisms underlying cerebellar circuit development mediated by the interplay between Cbln1/3 and GluRδ2.

Supplementary Material

Refer to Web version on PubMed Central for supplementary material.

Acknowledgments

Abbreviations

|	
AMPA	α-amino-3-hydroxy-5-methyl-4-isoxazone propionic acid
BSA	bovine serum albumin
CF	climbing fiber
DMEM	Dulbecco's modified Eagle's medium
ER	endoplasmic reticulum
HA	hemagglutinin
HEK293	Human embryonic kidney 293
HTBST	human serum albumin/0.1% Tween 20 in Tris-buffered saline
KO	knockout
PB	phosphate buffer
PBS	phosphate-buffered saline
PC	Purkinje cell
PF	parallel fiber
PSD	postsynaptic density
SDS-PAGE	sodium dodecyl sulfate-polyacrylamide gel electrophoresis
TBS	Tris-buffered saline
TNF	tumor necrosis factor

References

Albertin G, Malendowicz LK, Macchi C, Markowska A, Nussdorfer GG. Cerebellin stimulates the secretory activity of the rat adrenal gland: in vitro and in vivo studies. Neuropeptides. 2000; 34:7–11. [PubMed: 10688962]

Ayalon G, Stern-Bach Y. Functional assembly of AMPA and kainate receptors is mediated by several discrete protein-protein interactions. Neuron. 2001; 31:103–113. [PubMed: 11498054]

Bao D, Pang Z, Morgan JI. The structure and proteolytic processing of Cbln1 complexes. J Neurochem. 2005; 95:618–629. [PubMed: 16135095]

Bao D, Pang Z, Morgan MA, Parris J, Rong Y, Li L, Morgan JI. Cbln1 is essential for interaction-dependent secretion of Cbln3. Mol Cell Biol. 2006; 26:9327–9337. [PubMed: 17030622]

Berube NG, Swanson XH, Bertram MJ, Kittle JD, Didenko V, Baskin DS, Smith JR, Pereira-Smith OM. Cloning and characterization of CRF, a novel C1q-related factor, expressed in areas of the brain involved in motor function. Brain Res Mol Brain Res. 1999; 63:233–240. [PubMed: 9878755]

Bodmer JL, Schneider P, Tschopp J. The molecular architecture of the TNF superfamily. Trends Biochem Sci. 2002; 27:19–26. [PubMed: 11796220]

Burnet PW, Bretherton-Watt D, Ghatei MA, Bloom SR. Cerebellin-like peptide: tissue distribution in rat and guinea-pig and its release from rat cerebellum, hypothalamus and cerebellar synaptosomes in vitro. Neuroscience. 1988; 25:605–612. [PubMed: 3399060]

Craig AM, Kang Y. Neurexin-neuroligin signaling in synapse development. Curr Opin Neurobiol. 2007; 17:43–52. [PubMed: 17275284]

Fukaya M, Tsujita M, Yamazaki M, Kushiya E, Abe M, Akashi K, Natsume R, Kano M, Kamiya H, Watanabe M, Sakimura K. Abundant distribution of TARP gamma-8 in synaptic and extrasynaptic surface of hippocampal neurons and its major role in AMPA receptor expression on spines and dendrites. Eur J Neurosci. 2006; 24:2177–2190. [PubMed: 17074043]

Fukaya M, Watanabe M. Improved immunohistochemical detection of postsynaptically located PSD-95/SAP90 protein family by protease section pretreatment: a study in the adult mouse brain. J Comp Neurol. 2000; 426:572–586. [PubMed: 11027400]

Ferguson AR, Christensen RN, Gensel JC, Miller BA, Sun F, Beattie EC, Bresnahan JC, Beattie MS. Cell death after spinal cord injury is exacerbated by rapid TNFα-induced trafficking of GluR2-lacking AMPARs to the plasma membrane. J Neurosci. 2008; 28:11391–11400. [PubMed: 18971481]

Guastavino JM, Sotelo C, Damez-Kinselle I. Hot-foot murine mutation: behavioral effects and neuroanatomical alterations. Brain Res. 1990; 523:199–210. [PubMed: 2400906]

Hashimoto K, Ichikawa R, Takechi H, Inoue Y, Aiba A, Sakimura K, Mishina M, Hashikawa T, Konnerth A, Watanabe M, Kano M. Roles of glutamate receptor delta 2 subunit (GluRdelta 2) and metabotropic glutamate receptor subtype 1 (mGluR1) in climbing fiber synapse elimination during postnatal cerebellar development. J Neurosci. 2001; 21:9701–9712. [PubMed: 11739579]

Hirai H, Launey T, Mikawa S, Torashima T, Yanagihara D, Kasaura T, Miyamoto A, Yuzaki M. New role of delta2-glutamate receptors in AMPA receptor trafficking and cerebellar function. Nat Neurosci. 2003; 6:869–876. [PubMed: 12833050]

Hirai H, Pang Z, Bao D, Miyazaki T, Li L, Miura E, Parris J, Rong Y, Watanabe M, Yuzaki M, Morgan JI. Cbln1 is essential for synaptic integrity and plasticity in the cerebellum. Nat Neurosci. 2005; 8:1534–1541. [PubMed: 16234806]

Huttner WB, Schiebler W, Greengard P, De Camilli P. Synapsin I (protein I), a nerve terminal-specific phosphoprotein. III. Its association with synaptic vesicles studied in a highly purified synaptic vesicle preparation. J Cell Biol. 1983; 96:1374–1388. [PubMed: 6404912]

Ichikawa R, Miyazaki T, Kano M, Hashikawa T, Tatsumi H, Sakimura K, Mishina M, Inoue Y, Watanabe M. Distal extension of climbing fiber territory and multiple innervation caused by aberrant wiring to adjacent spiny branchlets in cerebellar Purkinje cells lacking glutamate receptor delta 2. J Neurosci. 2002; 22:8487–8503. [PubMed: 12351723]

Iijima T, Miura E, Matsuda K, Kamekawa Y, Watanabe M, Yuzaki M. Characterization of a transneuronal cytokine family Cbln--regulation of secretion by heteromeric assembly. Eur J Neurosci. 2007; 25:1049–1057. [PubMed: 17331201]

Innamorati G, Whang MI, Molteni R, Le Gouill C, Birnbaumer M. GIP, a G-protein-coupled receptor interacting protein. Regul Pept. 2002; 109:173–179. [PubMed: 12409230]

Ito-Ishida A, Miura E, Emi K, Matsuda K, Iijima T, Kondo T, Kohda K, Watanabe M, Yuzaki M. Cbln1 regulates rapid formation and maintenance of excitatory synapses in mature cerebellar Purkinje cells in vitro and in vivo. J Neurosci. 2008; 28:5920–5930. [PubMed: 18524896]

Kashiwabuchi N, Ikeda K, Araki K, Hirano T, Shibuki K, Takayama C, Inoue Y, Kutsuwada T, Yagi T, Kang Y, et al. Impairment of motor coordination, Purkinje cell synapse formation, and cerebellar long-term depression in GluR delta 2 mutant mice. Cell. 1995; 81:245–252. [PubMed: 7736576]

Kaul M, Loos M. Collagen-like complement component C1q is a membrane protein of human monocyte-derived macrophages that mediates endocytosis. J Immunol. 1995; 155:5795–5802. [PubMed: 7499868]

Kishore U, Gaboriaud C, Waters P, Shrive AK, Greenhough TJ, Reid KB, Sim RB, Arlaud GJ. C1q and tumor necrosis factor superfamily: modularity and versatility. Trends Immunol. 2004; 25:551–561. [PubMed: 15364058]

Kurihara H, Hashimoto K, Kano M, Takayama C, Sakimura K, Mishina M, Inoue Y, Watanabe M. Impaired parallel fiber-->Purkinje cell synapse stabilization during cerebellar development of mutant mice lacking the glutamate receptor delta2 subunit. J Neurosci. 1997; 17:9613–9623. [PubMed: 9391016]

Kuusinen A, Arvola M, Keinanen K. Molecular dissection of the agonist binding site of an AMPA receptor. Embo J. 1995; 14:6327–6332. [PubMed: 8557052]

Lalouette A, Lohof A, Sotelo C, Guenet J, Mariani J. Neurobiological effects of a null mutation depend on genetic context: comparison between two hotfoot alleles of the delta-2 ionotropic glutamate receptor. Neuroscience. 2001; 105:443–455. [PubMed: 11672610]

Landsend AS, Amiry-Moghaddam M, Matsubara A, Bergersen L, Usami S, Wenthold RJ, Ottersen OP. Differential localization of delta glutamate receptors in the rat cerebellum: coexpression with AMPA receptors in parallel fiber-spine synapses and absence from climbing fiber-spine synapses. J Neurosci. 1997; 17:834–842. [PubMed: 8987804]

Laube B, Hirai H, Sturgess M, Betz H, Kuhse J. Molecular determinants of agonist discrimination by NMDA receptor subunits: analysis of the glutamate binding site on the NR2B subunit. Neuron. 1997; 18:493–503. [PubMed: 9115742]

Lorincz A, Nusser Z. Specificity of immunoreactions: the importance of testing specificity in each method. J Neurosci. 2008; 28:9083–9086. [PubMed: 18784286]

Mazzocchi G, Andreis PG, De Caro R, Aragona F, Gottardo L, Nussdorfer GG. Cerebellin enhances in vitro secretory activity of human adrenal gland. J Clin Endocrinol Metab. 1999; 84:632–635. [PubMed: 10022429]

Miura E, Iijima T, Yuzaki M, Watanabe M. Distinct expression of Cbln family mRNAs in developing and adult mouse brains. Eur J Neurosci. 2006a; 24:750–760. [PubMed: 16930405]

Miura E, Fukaya M, Sato T, Sugihara K, Asano M, Yoshioka K, Watanabe M. Expression and distribution of JNK/SAPK-associated scaffold protein JSAP1 in developing and adult mouse brain. J Neurochem. 2006b; 97:1431–1446. [PubMed: 16606357]

Miyagi Y, Yamashita T, Fukaya M, Sonoda T, Okuno T, Yamada K, Watanabe M, Nagashima Y, Aoki I, Okuda K, Mishina M, Kawamoto S. Delphilin: a novel PDZ and formin homology domain-containing protein that synaptically colocalizes and interacts with glutamate receptor delta 2 subunit. J Neurosci. 2002; 22:803–814. [PubMed: 11826110]

Morgan JI, Slemmon JR, Danho W, Hempstead J, Berrebi AS, Mugnaini E. Cerebellin and related postsynaptic peptides in the brain of normal and neurodevelopmentally mutant vertebrates. Synapse. 1988; 2:117–124. [PubMed: 3420533]

Mugnaini E, Dahl AL, Morgan JI. Cerebellin is a postsynaptic neuropeptide. Synapse. 1988; 2:125–138. [PubMed: 3420534]

Nakagawa S, Watanabe M, Isobe T, Kondo H, Inoue Y. Cytological compartmentalization in the staggerer cerebellum, as revealed by calbindin immunohistochemistry for Purkinje cells. J Comp Neurol. 1998; 395:112–120. [PubMed: 9590549]

Ottersen OP, Landsend AS. Organization of glutamate receptors at the synapse. Eur J Neurosci. 1997; 9:2219–2224. [PubMed: 9464917]

Pang Z, Zuo J, Morgan JI. Cbln3, a novel member of the precerebellin family that binds specifically to Cbln1. J Neurosci. 2000; 20:6333–6339. [PubMed: 10964938]

Passafaro M, Nakagawa T, Sala C, Sheng M. Induction of dendritic spines by an extracellular domain of AMPA receptor subunit GluR2. Nature. 2003; 424:677–681. [PubMed: 12904794]

Rucinski M, Albertin G, Spinazzi R, Ziolkowska A, Nussdorfer GG, Malendowicz LK. Cerebellin in the rat adrenal gland: gene expression and effects of CER and [des-Ser1]CER on the secretion and growth of cultured adrenocortical cells. Int J Mol Med. 2005; 15:411–415. [PubMed: 15702230]

Saglietti L, Dequidt C, Kamieniarz K, Rousset MC, Valnegri P, Thoumine O, Beretta F, Fagni L, Choquet D, Sala C, Sheng M, Passafaro M. Extracellular interactions between GluR2 and N-cadherin in spine regulation. Neuron. 2007; 54:461–477. [PubMed: 17481398]

Shapiro L, Love J, Colman DR. Adhesion molecules in the nervous system: structural insights into function and diversity. Annu Rev Neurosci. 2007; 30:451–474. [PubMed: 17600523]

Shapiro L, Scherer PE. The crystal structure of a complement-1q family protein suggests an evolutionary link to tumor necrosis factor. Curr Biol. 1998; 8:335–338. [PubMed: 9512423]

Slemmon JR, Blacher R, Danho W, Hempstead JL, Morgan JI. Isolation and sequencing of two cerebellum-specific peptides. Proc Natl Acad Sci U S A. 1984; 81:6866–6870. [PubMed: 16593526]

Slemmon JR, Danho W, Hempstead JL, Morgan JI. Cerebellin: a quantifiable marker for Purkinje cell maturation. Proc Natl Acad Sci U S A. 1985; 82:7145–7148. [PubMed: 3863144]

Slemmon JR, Goldowitz D, Blacher R, Morgan JI. Evidence for the transneuronal regulation of cerebellin biosynthesis in developing Purkinje cells. J Neurosci. 1988; 8:4603–4611. [PubMed: 3199194]

Stellwagen D, Malenka RC. Synaptic scaling mediated by glial TNF-α. Nature. 2006; 440:1054–1059. [PubMed: 16547515]

Stern-Bach Y, Bettler B, Hartley M, Sheppard PO, O'Hara PJ, Heinemann SF. Agonist selectivity of glutamate receptors is specified by two domains structurally related to bacterial amino acid-binding proteins. Neuron. 1994; 13:1345–1357. [PubMed: 7527641]

Takeuchi T, Miyazaki T, Watanabe M, Mori H, Sakimura K, Mishina M. Control of synaptic connection by glutamate receptor delta2 in the adult cerebellum. J Neurosci. 2005; 25:2146–2156. [PubMed: 15728855]

Takeuchi T, Ohtsuki G, Yoshida T, Fukaya M, Wainai T, Yamashita M, Yamazaki Y, Mori H, Sakimura K, Kawamoto S, Watanabe M, Hirano T, Mishina M. Enhancement of both long-term depression induction and optokinetic response adaptation in mice lacking delphilin. PLoS ONE. 2008; 3:e2297. [PubMed: 18509461]

Urade Y, Oberdick J, Molinar-Rode R, Morgan JI. Precerebellin is a cerebellum-specific protein with similarity to the globular domain of complement C1q B chain. Proc Natl Acad Sci U S A. 1991; 88:1069–1073. [PubMed: 1704129]

Watanabe M. Molecular mechanisms governing competitive synaptic wiring in cerebellar Purkinje cells. Tohoku J Exp Med. 2008; 214:175–190. [PubMed: 18323688]

Watanabe M, Fukaya M, Sakimura K, Manabe T, Mishina M, Inoue Y. Selective scarcity of NMDA receptor channel subunits in the stratum lucidum (mossy fibre-recipient layer) of the mouse hippocampal CA3 subfield. Eur J Neurosci. 1998; 10:478–487. [PubMed: 9749710]

Wei P, Smeyne RJ, Bao D, Parris J, Morgan JI. Mapping of Cbln1-like immunoreactivity in adult and developing mouse brain and its localization to the endolysosomal compartment of neurons. Eur J Neurosci. 2007; 26:2962–2978. [PubMed: 18001291]

Yiangou Y, Burnet P, Nikou G, Chrysanthou BJ, Bloom SR. Purification and characterisation of cerebellins from human and porcine cerebellum. J Neurochem. 1989; 53:886–889. [PubMed: 2760624]

Yuzaki M. Cbln and C1q family proteins: new transneuronal cytokines. Cell Mol Life Sci. 2008; 65:1698–1705. [PubMed: 18278437]
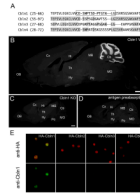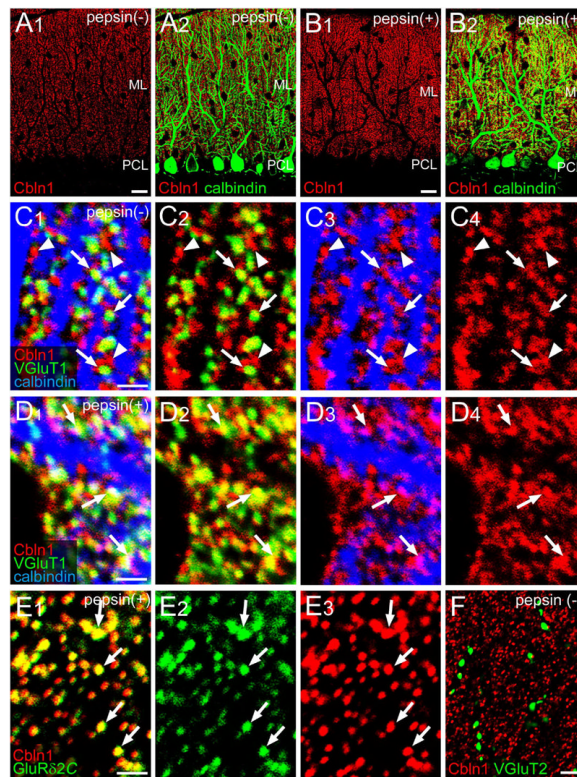
Figure 1.
Production and specificity of Cbln1 antibody. (A) Sequence alignment of antigen region of the Cbln family. Boxed sequence is selected for antigen of Cbln1 antibody production (38-52 amino acid residues), and is low in homology with other Cbln members. (B-D) Single immunofluorescence with use of rabbit Cbln1 antibody in the brain of wild-type mice (B and D) and Cbln1-KO mice (C). In D, Cbln1 antibody preabsorbed with antigen peptide was used. (E) Specificity of anti-Cbln1 antibody to Cbln1. HA-tagged Cbln1-Cbln4 were expressed in HEK293 cells and immunoreactivity was analyzed using anti-Cbln1 (green) and anti-HA (red) antibodies. Cb, cerebellum; Cx, cortex; Hi, hippocampus; Hy, hypothalamus; MB, midbrain; MO, medulla oblongata; OB, olfactory bulb; Po, pontine nucleus; Th, thalamus. Scale bars, 1 mm.
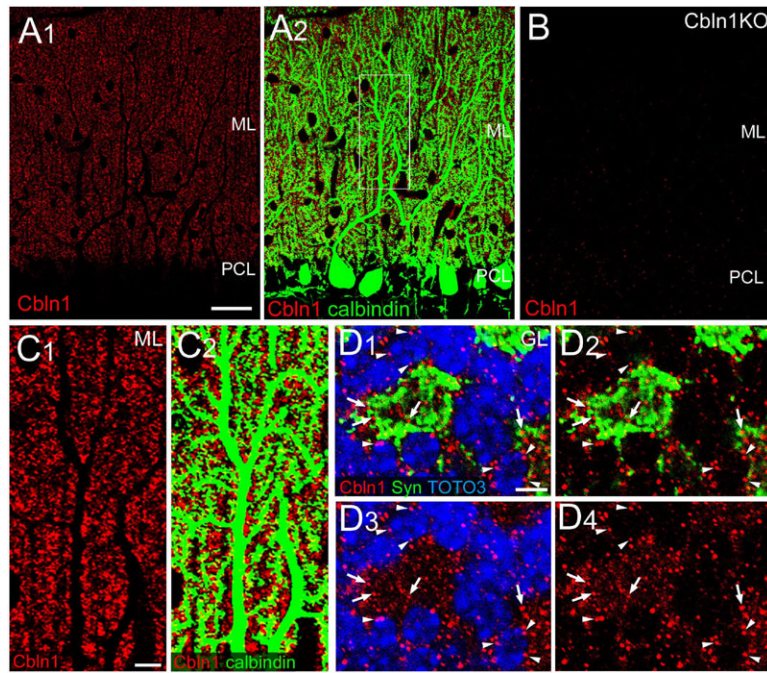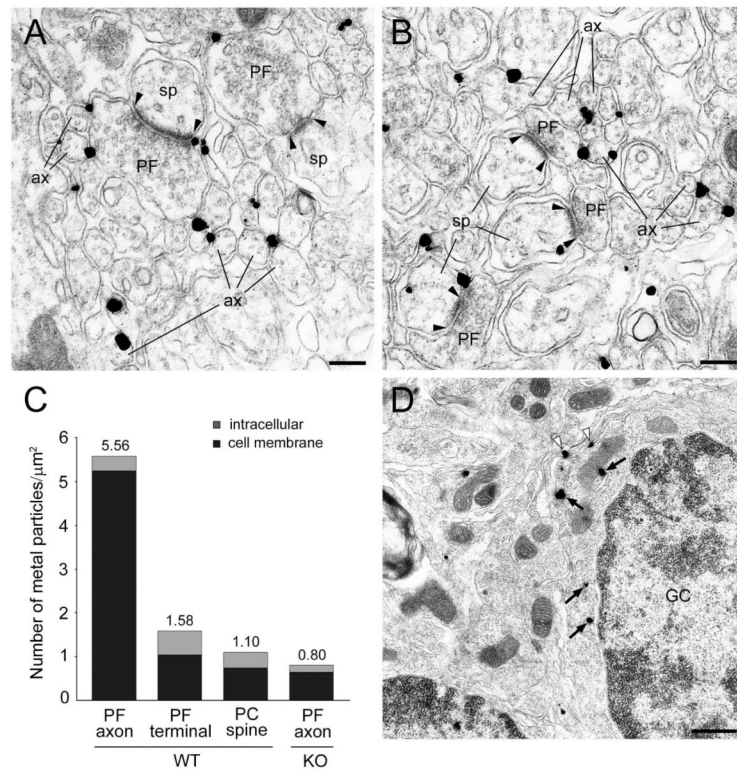
Figure 2.
Distribution of Cbln1 in the cerebellar cortex. (A and C) Double immunofluorescence for Cbln1 (red) and calbindin (green). C shows an enlarged image of a boxed region in A. (B) Single immunofluorescence for Cbln1 in the Cbln1-KO mouse. (D) Triple immunofluorescence for Cbln1 (red), synaptophysin (syn; green), and TOTO-3 (blue, nuclear staining) in the cerebellar granular layer. Arrows and arrowheads indicate punctate Cbln1 signals in synaptic glomeruli and perikarya of granule cells, respectively. GL, granular layer; ML, molecular layer; PLC, Purkinje cell layer. Scale bars, 30 μm (A and B); 10 μm (C); and 5 μm (D).
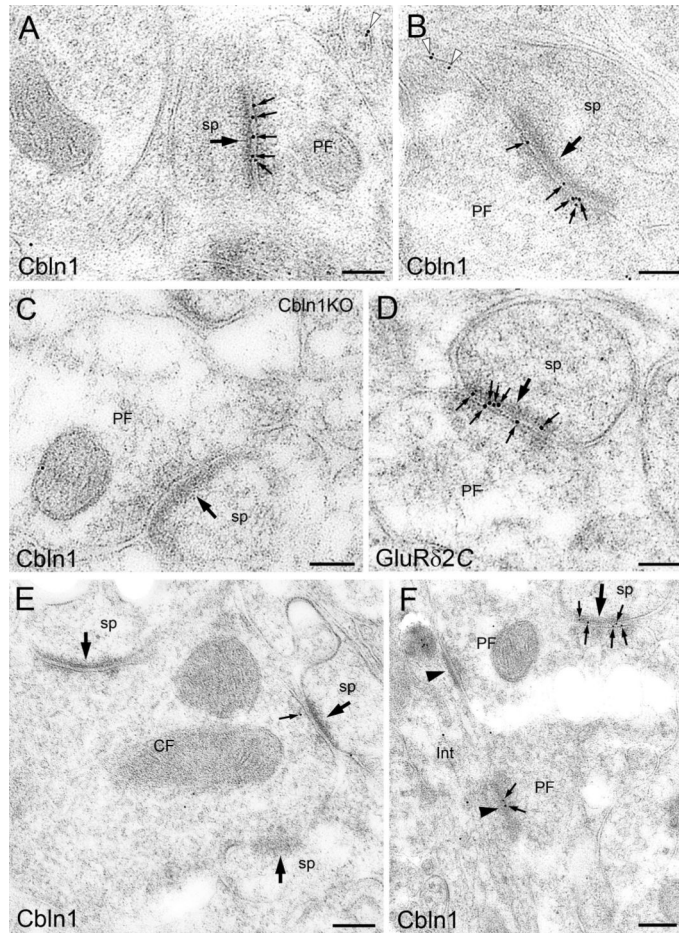
Figure 3.
Cbln1 immunofluorescence in the cerebellar molecular layer before (A, C, and F) and after (B, D, and E) pepsin pretreatment. Cbln1 is pseudocolored in red, while other markers are in green or blue. (A and B) Single (A1 and B1) or double (A2 and B2) staining for Cbln1 and calbindin (green) at low magnification. (C and D) Triple staining for Cbln1, VGluT1 (green), and calbindin (blue) at high magnification. Arrows indicate relatively weak Cbln1 puncta that are overlapped with VGluT1. Arrowheads indicate intense Cbln1 puncta that are not overlapped with either VGluT1 or calbindin. (E) Double staining for Cbln1 and GluRδ2C (green) showing their almost complete overlap (arrows). (F) Double staining for Cbln1 and VGluT2 (green) showing little or no Cbln1 expression in VGluT2-positive climbing fiber terminals. GL, granular layer; ML, molecular layer; PLC, Purkinje cell layer. Scale bars, 20 μm (A and B); 2 μm (C-E); and 5 μm (F).

Figure 4.
Distribution of Cbln1 in the cerebellar molecular layer by silver-enhanced immunoelectron microscopy. (A and B) Metal particles for Cbln1 were detected on the cell membrane of PFs and PC spines in wild-type mice. Arrowheads indicate the edge of postsynaptic density (PSD). (C) Histogram shows the density of immunogold labeling for Cbln1 in PFs and PC dendrites and spines. The densities of particles associated with the cell membrane (dark gray) and in intracellular sites (pale gray) are 5.22 and 0.34 in non-terminal PF axons, 1.04 and 0.54 in PF terminals, and 0.74 and 0.36 in PC spines in wild-type mice, while that in non-terminal PF axons of Cbln1-KO mice is 0.64 or 0.16, respectively. The total area of measured elements is 76.65 μm^2 for non-terminal PF axons, 35.35 μm^2 for PF terminals, and 19.59 μm^2 for PC spines in wild-type mice, and 31.16 μm^2 in non-terminal PF axons of Cbln1-KO mice. (D) Metal particles for Cbln1 were detected in perikarya of granule cells. Arrows and open arrowheads indicate signals in the cytoplasm and on the cell membrane, respectively. Scale bars, 200 nm (A and B); 500 nm (D).
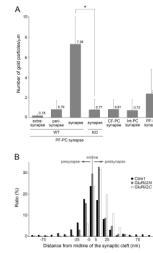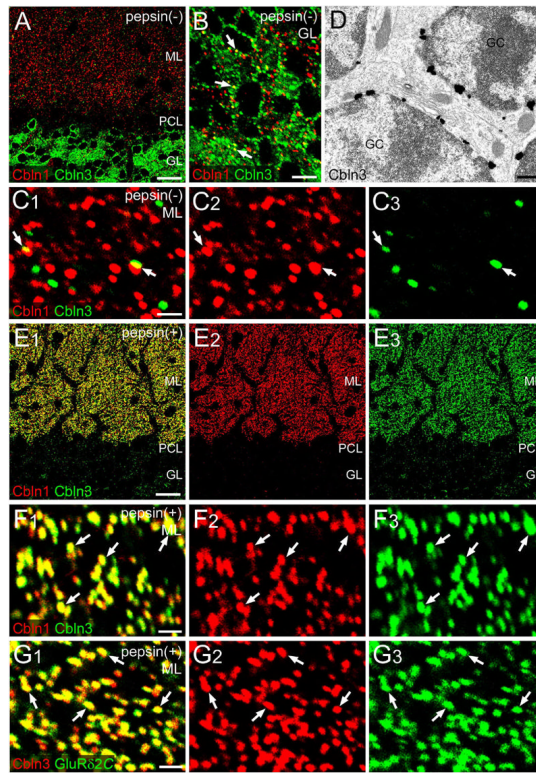
Figure 5.
Postembedding immunogold electron microscopy showing almost selective labeling for Cbln1 (A-C, E, and F) and GluRδ2*C* (D) at PF synapses. Large allows indicate postsynaptic density (PSD) of PC spines contacted to PF terminals (A-D and F) or CF ones (E). Small arrows and open arrowheads indicate synaptic or extrasynaptic labeling, respectively. (A and B) Intense labeling at the PF-PC synapse of wild-type mice. (C) No significant labeling at the PF-PC synapse of Cbln1-KO mice. (D) Intense labeling with GluRδ2*C* antibody at the PF-PC synapse. (E) No significant labeling at the climbing fiber (CF)-PC synapse. (F) Occasional low labeling at the PF-interneuron (Int) synapse (filled arrowheads). sp, spine. Scale bars, 200 nm.

Figure 6.
Quantification of postembedding immunogold labeling. (A) Histogram showing the density of immunogold labeling for Cbln1 on the extrasynaptic (> 100 nm apart from the synaptic edge), perisynaptic (< 100 nm), and synaptic (between two synaptic edges) membranes of the PF-PC synapse, and on the synaptic membranes of the climbing fiber (CF)-PC synapse, interneuron (Int)-PC synapse, and PF-interneuron synapse. The background level was determined from synaptic labeling at the PF-PC synapse of Cbn1-KO mice. The total length of measured cell membrane at the PF-PC synapse is 231.93 μm for the extrasynapse (n = 46 gold particles in total), 37.40 μm for the perisynapse (30 particles), and 60.74 μm for the synapse in wild-type mice (422 particles in 258 synapses), and 21.05 μm for the synapse in Cbln1-KO mice (17 particles in 87 synapses). The total length of measured cell membrane is 5.96 μm for the CF-PC synapse (6 particles in 23 synapses), 8.65 μm in the Int-PC synapse (7 particles in 40 synapses), and 7.56 μm in the PF-Int synapse (17 particles in 38 synapses). Bars on each column represent SD. *, p < 0.001; unpaired Student's *t*-test. (B) Histogram showing the vertical distribution of Cbln1 and GluRδ2 epitopes at the PF-PC synapse. The distance was measured from the midline of the synaptic cleft to the center of immunogold particles. In the x-axis, minus and plus represent presynaptic or postsynaptic side, respectively, from the midline. The total number of counted immunogold particles is 1145 for Cbln1, 690 for GluRδ2*N*, and 709 for GluRδ2*C*.

Figure 7.
Distribution of Cbln3 in relation with Cbln1 and GluRδ2 in the cerebellum. (A-C) Double staining for Cbln1 (red) and Cbln3 (green) without pepsin pretreatment. Cbln1 and Cbln3 are overlapped in a few puncta (arrows in B, C). (D) Preembedding silver-enhanced immunogold electron microscopy for Cbln3 in granule cells (GCs). (E and F) Double staining for Cbln1 (red) and Cbln3 (green) after pepsin pretreatment. Cbln3 labeling is almost completely overlapped with Cbln1, yielding yellowish puncta (arrows). Because the picture E was taken by lowering the gain level of confocal microscope in order to adjust it to the intensified puncta in the molecular layer, Cbln3 labeling in the granular layer is greatly reduced, as compared to A. (G) Double staining for Cbln3 (red) and GluRδ2C (green) after pepsin pretreatment. Cbln3 is almost completely overlapped with GluRδ2 (arrows). GL, granular layer; ML, molecular layer; PLC, Purkinje cell layer. Scale bars, 20 μm (A and E); 5 μ□ (B); 2 μ, (C, F, and G); 500 nm (D).